Active reduction of sound transmission through triple panel partitions: performance evaluation

I. Dimino[a)]
A. Concilio[b)]
CIRA, the Italian Aerospace Research Centre
Via Maiorise
81043 Capua (CE) Italy

A. Pierré[c)]
University of Technology of Belfort-Montbéliard, Belfort, France

M. H. Aliabadi[d)]
Imperial College, Department of Aeronautics, South Kensington Campus, London, United Kingdom

This paper deals with the development of a multi-channel ASAC controller for reducing sound transmission through triple panel partitions. The X-filtered version of the adaptive least mean squares (LMS) algorithm is implemented by utilizing up to eight (stack) piezoelectric actuators as control inputs and four microphones located in the radiated field as error sensors. The control signals to piezoelectric actuators are computed on the base of the noise signals measured at the error sensors. This approach is particularly useful for periodic noise disturbances, like propeller-induced noise for a turboprop aircraft, because they can be perfectly synchronised to the BPF. In addition, as an alternative to the multichannel version of the filtered-X LMS algorithm, the least maximum mean squares (LMMS) and the Scanning-error LMS algorithms are investigated in order to control different types of primary sound fields. Harmonic disturbances till flat band-limited white noise excitations are considered. A variety of cases are studied by varying the number of control actuators to evaluate the amount of achievable attenuation.

[a)] email: i.dimino@cira.it
[b)] email: a.concilio@cira.it
[c)] email: andrea.pierre@assidu-utbm.fr
[d)] email: m.h.aliabadi@imperial.ac.uk

1 INTRODUCTION

The advent of integrated circuits and the rapid development of cost-effective digital signal processing (DSP) chips have enabled digital active control technology to emerge as practical alternative to passive treatments in aircraft applications. Active control solutions are potentially most effective at low frequencies where conventional, passive, noise control means cannot generally be applied without weight and space penalties.

The implementation of multichannel systems, based on multi-input-multi-output (MIMO) controllers, has proved to be effective for controlling both periodic and broadband noise. However, memory requirements and computation loads as well as the mutual interaction between error microphones and secondary sources limit the performance of such a type of control on large systems. A multichannel active noise control system for broadband noise disturbances has been tested on a light jet aircraft to enhance cabin comfort, [1]. In [2], a controller design method to optimize loudspeaker and microphone positions in a narrow-band system is presented to achieve a global noise reduction inside an aircraft passenger cabin. In order to create a zone of quiet around the passenger's head, relatively large loudspeaker arrangements are used.

Additionally, a considerable amount of studies involving active acoustic control of vibrating plates has been published over the last fifteen years. Such systems are focused on controlling acoustically radiating modes either by using point force inputs directly attached to the structure instead of imposing a secondary, loudspeaker-generated sound field. Active structural-acoustic control is then achieved by modal suppression, meaning that during control, all the modal amplitudes are reduced, or by modal restructuring leading to a residual structural response with lower radiation efficiency. In [3], active control of simple plate structures is investigated by utilizing surface sensors (PVDF) to estimate the acoustic radiation and piezoelectric elements as control inputs. However, since the desired goal is to reduce the radiated sound field, the use of acoustic transducers as error sensors may increase the effectiveness of the control strategy.

Due to the highly correlated reference signal which is accessible by monitoring the engines, active noise reduction in propeller aircraft has been a typical subject of feed-forward control. With the advances in adaptive structures, this approach has been extended to ASAC applications by focusing on sensing and actuation integration within the structure. For jet aircraft, instead, reliable control strategies are yet to be demonstrated since many complex sources such as boundary layer noise and jet noise are involved in creating the disturbance in the cabin.

In this paper, an adaptive feed-forward multichannel control algorithm is designed for local active noise control at error sensors. The adaptive control system consists of two main parts: a number of digital filters which are adjusted by means of an adaptive algorithm capable of tracking variations in the noise radiation characteristics. The reference signal is taken directly from the primary source. This set-up is a somewhat "idealized" arrangement and, in general, will yield some kind of best results suitable to evaluate the benefits of active control in multi-panel partitions.

2 PANEL CONTROL OF A TRIPLE PANEL PARTITION

Due to the fluid-structure interaction, transmission loss of multi wall structures suffers the unfavorable effects of resonant noise transmission. At a certain frequency, known as the mass-air-mass resonance, the airspace, which acts like a spring between the partitions, dynamically couples the masses of the partitions, thus increasing the sound transmission in comparison to an equivalent single panel. Although this phenomenon occurs in a limited frequency range, it causes significant drops in the sound transmission loss behaviour.

In order to meet reduced cabin noise targets, the vibro-acoustic tailoring of fuselage panels containing windows may be particularly important, especially in turboprop aircraft. Although windows may compromise only 5 to 10 percent of the sidewall area, they are a privileged path for structure-borne and air-borne noise transmission into cabin, [4, 5]. Since the propeller-induced acoustic excitation occurs in the very low frequency range, such a reduced sound transmission loss properties result in higher interior noise levels, which are often considered highly annoying to a large percentage of passengers.

Active control of aircraft transparent windows through piezoelectric actuators may represent a viable technology to reduce the sound transmission through aircraft fuselage panels. To this aim, the position of the control actuators must be chosen so that their influence on vibro-acoustic modes with higher radiation efficiency is expected to be optimal. However, among the possible actuator locations, the piezoelectric actuators must not interfere with the primal function of the controlled structure, namely to look through.

In this paper, an effective solution for actively controlling sound transmission through triple panel windows is investigated. The control mechanism is based on segmented actuators placed at the borders of the radiating panel. A sketch of the actuation mechanism is shown in Fig. 1. The smart window is modelled and manufactured rectangular and flat for ease of fabrication and testing. Obviously, the resulting design is a strongly simplified model of an actual aircraft window. Nevertheless, this assumption is consistent with the literature available for double and triple wall partitions, largely investigated as homogeneous and flat panel systems [6]. A detailed description of the model is provided in [7]. The investigated triple panel partition consists of three parallel and transparent window panes with an area of 32 x 20 cm, an aluminium frame and two enclosed cavities, as shown in Fig. 2. Two of the three panes are made of 0,94 cm thick glass and are separated by an airspace d_1 of 1,66 cm. The third pane, which is made of acrylic, is 0,64 cm thick and it is separated from the closest glass pane by a 3,62 cm airspace d_2. The material properties are listed in table 1. The panes are supported by strips of elastomer and they can freely rotate. A silicon rubber is used to secure the window in the aluminium frame. Ten COTS piezoelectric stack actuators are used to control the radiating panel of the window, as shown in Fig. 1. The piezoelectric actuators are distributed along the window frame in order to provide in-plane forces on the radiating panel of the window by taking advantage of the d_{33} effect. In this configuration, each piezo actuator generates off-midplane actuation forces on the radiating pane inducing local bending moments aiming at controlling the out-of-plane vibro-acoustic radiation. These dynamic forces are transferred to the plexiglas panel through metal rods, which keep the piezoceramic actuators in their compressive state when no voltage is present. This solution allows to decouple the incident and the radiating panel vibrations. In addition, it permits to control the flexural modes effectively, by controlling independently the driving voltage applied to each actuator. This cannot be executed if the actuators are continuous over the length of the structure. By configuring the actuators as a distributed “active boundary”, the direct sound radiation can thus be effectively controlled. Furthermore, from a more practical point of view, the structural actuators can be easily hidden in the frame of the window.

3 EXPERIMENTAL SYSTEM IDENTIFICATION

With the recent advances in computer technology for data acquisition, signal processing and analysis, plant models necessary to test active noise control performance can be identified accurately from the measured responses and excitations using system identification techniques.

In this work, the noise transmission path from the exterior to the interior of an aircraft sidewall panel is simplified through an experimental arrangement aimed at characterizing the sound transmission properties of a smart window prototype. Such a representative set-up is shown in Fig. 3. It consists of two parts: a soundproof box and the triple wall test-bed mounted on the side opening of the box. The incident acoustic field which is simulated for this study is the noise generated by the propeller of a turboprop aircraft approximated by acoustical oblique incident sound waves. Such a primary noise source is experimentally generated by a loudspeaker placed inside the box. The radiated acoustic field of the window panels corresponds to the aircraft interior which is approximated by an acoustical free field. The transmitted noise is measured within a semi-anechoic chamber.

The control signals to the piezoelectric actuators are computed by the filtered-reference LMS control theory. The governing equations are described in Section 4. Due to the better coherence with the radiated sound field, sound pressure sensors on the radiating side of the vibrating structure are used as error signals. The experimental plants, relating the input and output of the system under control, have been recorded off-line, before the control system operation.

The experimental plant responses have been measured for both the disturbing noise source and the active window prototype driven by the control actuators. Next, they have been numerically fitted and integrated in the active noise control algorithm. The acoustic field emitted by the loudspeaker has been characterized in the 50-800 Hz frequency range. Band limited white noise has been used as noise disturbance. No. 4 microphones have been placed in the receiving room in order to measure the respective transfer functions, as shown in Fig. 4. The fitting of the experimental curves has been realized by using the MATLAB “invfreqs” function from the Signal Processing Toolbox. The fitting coefficients matching the experimental data have been then converted in a state-space model:

$$\begin{aligned} \dot{x} &= Ax + Bu \\ y &= Cx + Du \end{aligned} . \tag{1}$$

Fig. 5 shows the acoustic plants for the mics no.2 and no. 3 measured by driving the primary noise source within the sending room. The fitted transfer functions are then compared with the experimental ones. A perfect agreement in magnitude and phase has been achieved between the numerical and experimental data.

4 MULTICHANNEL ADAPTIVE CONTROL

The multichannel version of the filtered-X LMS algorithm is called the multiple error LMS algorithm (MELMS). Considering K reference signals, M secondary sources and L error sensors, the output of the l-th error sensor can be written as

$$e_l(n) = d_l(n) + \sum_{k=1}^{K}\sum_{m=1}^{M}\sum_{j=0}^{J-1} c_{lmj} \sum_{i=0}^{I-1} w_{mki} x_k(n-i-j) . \tag{2}$$

where $d_l(n)$ is the primary noise at the lth error sensor, c_{lmj} is the jth coefficient of the impulse response from the mth secondary source to the lth error sensor. The signal driving the mth actuator is obtained by the contribution from K reference signals, each filtered by an Ith order FIR control filter with coefficient w_{mki}. Equation (2) can also be expressed in matrix form as

$$\mathbf{e}(n) = \mathbf{d}(n) + \mathbf{R}(n)\mathbf{w} . \tag{3}$$

where

$$\mathbf{e}(n) = [e_1(n), e_2(n), \cdots, e_L(n)]^T \,. \tag{4}$$

$$\mathbf{d}(n) = [d_1(n), d_2(n), \cdots, d_L(n)]^T \,. \tag{5}$$

$$\mathbf{w} = [\mathbf{w_o}^T, \mathbf{w}_1^T, \cdots, \mathbf{w}_{I-1}^T]^T \,. \tag{6}$$

with

$$\mathbf{w}_i = [w_{11i}, w_{12i}, \cdots, w_{1Ki}, w_{21i}, \cdots, w_{MKi}]^T \,. \tag{7}$$

$$\mathbf{R}(n) = \begin{bmatrix} \mathbf{r}_1^T(n) & \mathbf{r}_1^T(n-1) & \cdots & \mathbf{r}_1^T(n-I-1) \\ \mathbf{r}_2^T(n) & \mathbf{r}_2^T(n-1) & \cdots & \mathbf{r}_2^T(n-I-1) \\ \vdots & & & \\ \mathbf{r}_L^T(n) & \mathbf{r}_L^T(n-1) & & \mathbf{r}_L^T(n-I-1) \end{bmatrix} . \tag{8}$$

$$\mathbf{r}_l(n) = [r_{l11}(n), r_{l12}(n), \cdots, r_{l1K}(n), r_{l21}(n), \cdots, r_{lMK}(n)]^T \tag{9}$$

According to the multifiltered-X LMS algorithm, the control filter coefficients of the multichannel algorithm may be adjusted iteratively at every sample time by an amount proportional to the negative instantaneous value of the stochastic estimation of the gradient vector. The vector of derivatives of the instantaneous squared errors with respect to the control coefficients is given by

$$\frac{\partial \mathbf{e}^T(n)\mathbf{e}(n)}{\partial \mathbf{w}(n)} = 2\mathbf{R}^T(n)\mathbf{e}(n) \tag{10}$$

Equation (12) yields the well-known adaptation algorithm

$$\mathbf{w}(n+1) = \mathbf{w}(n) - \alpha \mathbf{R}^T(n)\mathbf{e}(n) \tag{11}$$

where α is a convergence coefficient.

For large multi-channel systems, the filtered-x operations of the reference signals require intensive computations. An alternative method for reducing the computational load of the multichannel filtered-X LMS algorithm consists of using only one error signal at each algorithm iteration to adapt all the filter coefficients. In the Least Maximum Mean Squares (LMMS) algorithm, the stochastic cost function consists of the instantaneous maximum value of the error signals. Another method for reducing the computation load is the scanning error-LMS algorithm. In this case, the error signal is chosen in turn at each algorithm iteration. An interesting analysis of the computational complexity of multichannel systems, such as MELMS, LMMS and Scanning-error is reported in [8]. Unlike the MELMS and LMMS, the scanning-error algorithm does not depend on the number of error sensors and requires much fewer operations per sampling period.

5 NUMERICAL SIMULATIONS

This section theoretically investigates the active noise reduction that can be achieved with a predetermined configuration of secondary sources mounted on the smart panels using a feedforward control scheme. The aim is, firstly, to show the potential of active control to improve the sound insulation of triple panel systems and, secondly, to give a comprehensive overview of the physical system under investigation. Sound radiation is numerically addressed with and without control by performing feedforward simulations.

The direct control of the radiating surface of the triple panel system is achieved by using a set of d_{33} piezo actuators introducing secondary control signals into the smart panels. A multichannel active noise control is used to attenuate the sound field radiated by the vibrating panel. Due to the better coherence with the radiated sound field, sound pressure sensors on the radiating side of the vibrating structure are used as error signals.

For the primary acoustic excitation, different incident sound fields are considered. First, the adaptive feedforward control is tested against transient noise signals varying between 80 and 140 Hz in order to simulate a slightly varying BPF due to a maneuvering flight. Moreover, flat random noise is added to the harmonic noise disturbance in order to achieve a predetermined signal-to-noise ratio representative of a more realistic noise level. Second, the system is excited by a random broadband excitation rather than single harmonic frequencies.

In order to control band-limited noise excitations, three different adaptive signal processing algorithms are used. They are: multichannel filtered-X LMS (MELMS), least maximum mean squares (LMMS) and scanning error-LMS algorithms. They are steepest descent-type algorithms which have shown to be robust and of low computational complexity. The block diagram of the control loop is illustrated in Fig. 6. One reference signal is considered.

The control algorithms are tested at different error sensor positions. The noise reduction in the area close to the triple panel system is investigated by placing the error sensors at a distance of 100 mm, 150 mm, 700 mm and 1050 mm respectively from the surface of the radiating panel. The first two acoustic sensors have a practical significance, as people have to stay close to the window in aircraft cabin. The remaining error sensors are representative for noise reduction in the far field.

5.1 Narrow-band primary noise

In order to illustrate the capability of the developed algorithms to track variations in the primary noise characteristics, a narrow-band disturbance is considered. A bidirectional linear sweep ranging from 80 Hz to 140 Hz and whose frequency changing rate is 30 Hz/s (80 Hz to 140 Hz in 2 seconds, for both increasing and decreasing frequencies) is thus simulated. Such an acoustic excitation is chosen to replicate an engine run-up operation before aircraft take-off or the slight variation in the engine's rpm due to maneuvers. The application of an adaptive algorithm, consisting of four error sensors and four control actuators, allows to track these changes by updating the FIR filter coefficients.

The controllers are designed to adjust the amplitude and phase of the reference signal, whose sinusoidal frequency is arranged to be changing in time, in order to drive each secondary actuator properly. The adaptive control is tested by monitoring the behaviour of the filter coefficients with respect to the time-varying disturbance as well as by calculating the global noise attenuation achieved. Fig. 7 shows the numerical attenuations predicted by using the MELMS algorithm. The red signal and the green signal are respectively the noise disturbance and the control signal induced by the piezo-stack actuators to the radiating panel. The blue curve is the residual acoustic field obtained when the control system is engaged.

The time-frequency analysis of the primary noise disturbance is illustrated in Fig 8 (left). The frequency content of the signal changes between the lower and upper frequency limits of the swept sine. Fig. 8 (right) illustrates the spectrogram plot of the error signal at one of the error sensors with control. Such a spectogram is obtained by the average of the STFT of the signal

calculated at regular intervals of time (0.1 seconds). A flat random noise, whose frequency contribution can be observed, is added to the primary signal in order to simulate a more realistic acoustic disturbance. Although the control system performance is limited by such a random noise, a perceptible attenuation is achieved for all the error sensors. A mean reduction of 87,9 % in the disturbance signal is obtained at the sensor #2, corresponding to a noise attenuation of 18,40 dB in the overall sound pressure level. The reduction always remains important even in the other error sensors.
A comparison between the sound pressure levels obtained with and without control by the three different adaptive algorithms is listed in Table 2. No remarkable differences are achieved in the attenuation results. Notice that they are computed as the mean difference between the level of the acoustic field before and after the active control. A faster noise reduction is obtained by the MELMS algorithm as it uses all the error signals. On the other hand, the LMMS algorithm provides a more uniform residual field compared with the MELMS and Scanning-error LMS since such a control strategy is based on the minimization of the maximum error signal.

5.2 Random primary noise

Starting with a single channel control, a feedforward controller consisting of multiple secondary actuators and multiple error sensors is also investigated when the primary source is driven by a band-limited white noise signal in the range 112-562 Hz. The multichannel control systems use either one control output driving eight piezoelectric actuators in parallel (piezo 2, 3, 4, 5, 7, 8, 9 and 10), two control outputs driving two secondary sources (piezo 2 and 7) or four individual control channels (piezo 2, 5, 7 and 10) to reduce the acoustic pressure radiated in front of the panel. The number of the output control channels are used for the description of the results. In all three cases, the control performance associated with the minimisation of the pressure at the four error microphones is compared to the case when no control is applied.

In contrast to the results achieved with narrow-band control, sound attenuation is investigated over a broad-band frequency range. The stochastic character of the primary signal makes the active control more difficult with respect to the control of tonal frequencies. The measured spectra, compared with and without control, yield a rough estimate of the improvements in the insertion loss achievable by the actively controlled structure. In Fig. 9, the results of the adaptive feedforward control are shown by considering a MELMS algorithm with 512 coefficients. The magnitude of the noise radiation detected by the acoustic sensor is reduced significantly throughout the third-octave bands of noise.

The sound attenuation tends to improve with an increasing number of controlled secondary actuators. If all eight piezo actuators are driven equally through a single output controller, the sound radiation is reduced by 13 dB around the first resonance. A higher attenuation is observed for higher frequencies up to 300 Hz, if two secondary sources are used to attenuate the response at the error sensors. By extending the number of control actuators to four, the performance is significantly increased. This means that the higher the modal density in the frequency band of interest, the higher the number of actuators which are required to capture the radiation characteristics of the panel.

Fig. 10 shows the third-octave band results obtained for the MELMS, LMMS and Scanning error-LMS algorithms before and after the controller system operations. The noise reduction levels are obtained by averaged noise spectra calculated by subdividing the time-domain signals into 200 millisecond blocks. The results achieved for the three cases show meaningful reductions in the band-limited white noise excitation at the sensor positions for all the working frequencies. The profile of the sound pressure level spectra represents a good reference point to predict the quiet zone obtainable with four control actuators. The MELMS and LMMS algorithms succeed in globally reducing acoustic pressure at microphones with higher levels. However, the LMMS algorithm achieves more uniform final levels at the expense of an increase in the mean square values of the individual error signals. Attenuation higher than 20 dB is achieved at some frequencies by using the scanning-error LMS algorithm. A very low convergence time, defined as the time at which the squared error falls below 10 % of its initial value, is obtained due to the very small values of alpha required to retain the algorithms stable.

6 CONCLUSIONS

The effectiveness of a multi-channel ASAC controller in suppressing the sound radiation from a triple panel active window test-bed is numerically investigated by using experimental plant models experienced on the field. It is assumed that the dynamic behavior of the system to be controlled does not change during control, and can be measured beforehand through experimental system identification techniques. Control structural inputs to the piezoelectric actuators are computed so as to reduce the radiated sound field. The signals driving the secondary actuators are obtained by properly filtering the reference signal via a digital controller. The control system performance is evaluated for narrow-band and broadband noise. Theoretical FIR filter coefficients able to suppress narrow-band primary noise between 80 and 140 Hz are calculated with and without adding random background noise to the imposed disturbance. A band-limited white noise excitation is also considered in the range 112-562 Hz. The derivation of three multi-input/multi-output controllers, namely the multichannel filtered-X LMS (MELMS), the Least Maximum Mean Squares (LMMS) and the Scanning error-LMS algorithms, is discussed for use in numerical simulation studies. Noise simulation results demonstrate that the insertion loss of the triple panel partition can be significantly improved by adaptively controlling the sound field monitored by external error sensors.

7 REFERENCES

1. O. Pabst, T. Kletschkowski, and D. Sachau. Active noise control in light jet aircraft. Journal of The Acoustical Society of America, 123, 2008.
2. T. Kletschkowski, D. Sachau, S. Bohme, and H. Breitbach. Optimized active noise control of semiclosed aircraft interiors. International Journal of Aeroacoustics, 6:61–71, 2007.
3. J. P. Maillard and C. R. Fuller. Active control of sound radiation from cylinders with piezoelectric actuators and structural-acoustic sensing. Journal of Sound and Vibration, 222:363–388, 1999.
4. L. Guillaumie, J.M. David, and O. Voisin Grall. Internal fuselage noise: comparison of computations and tests on a falcon airframe. Journal of Aerospace Science and Technology, 4(8):545–554, 2000.
5. R.E. Hayden, B.S. Murray, and M.A. Theobald. A study of interior noise levels, noise sources and transmission paths in light aircraft. NASA CR 172152, 1985.
6. R. A. Prydz and F. J. Balena. Window acoustic study for advanced turboprop aircraft. NASA CR 172391, 1984.
7. I. Dimino, A. Vigliotti, M.H. Aliabadi, A. Concilio, Vibro-acoustic design of an aircraft-type active Window, Part 1: dynamic modelling and experimental validation, Journal of Theorethical and Applied Mechanics, vol. 50, no. 1, pp. 169-192, 2012.
8. M. De Diego and A. Gonzalez. Performance evaluation of multichannel adaptive algorithms for local active noise control. Journal of Sound and Vibration, 244(4):615–634, 2001.

Table 1 – Material properties of the triple panel window.

Material	Young's modulus (GPa)	Poisson ratio	Density (kg/m^3)
Plexiglass	3.1	0.4	1190
Glass	62	0.24	2480
Elastomer	0.025	0.49	1300
Alluminium	72.4	0.33	2780

Table 2 – Noise attenuation achieved at the error microphones for a sweeping sine wave signal

	Sweeping sine wave disturbance [80-140] Hz		
	MELMS (dB)	LMMS (dB)	Scanning (dB)
Control mic. 2	18.40	17.52	18.86
Control mic. 3	16.33	15.78	16.27
Control mic. 4	10.80	11.85	10.94
Control mic. 5	4.91	5.65	5.26

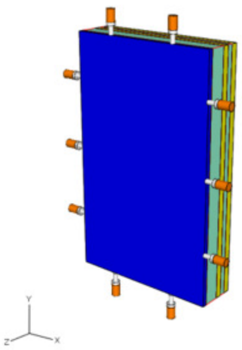

Fig. 1 Piezo actuators in the triple partition

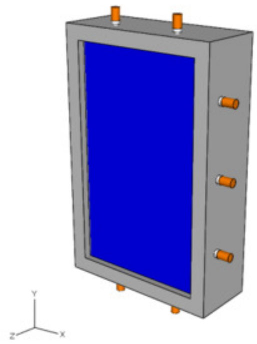

Fig. 2 Triple panel partition

Fig. 3 – View of the experimental set-up from the receiving room.

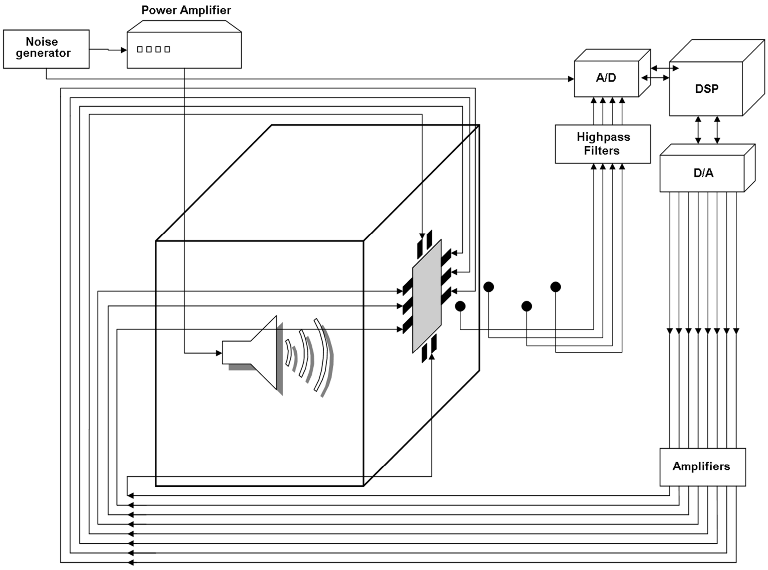

Fig. 4 – Schematic presentation of the experimental set-up with the smart window prototype mounted on the testing facility.

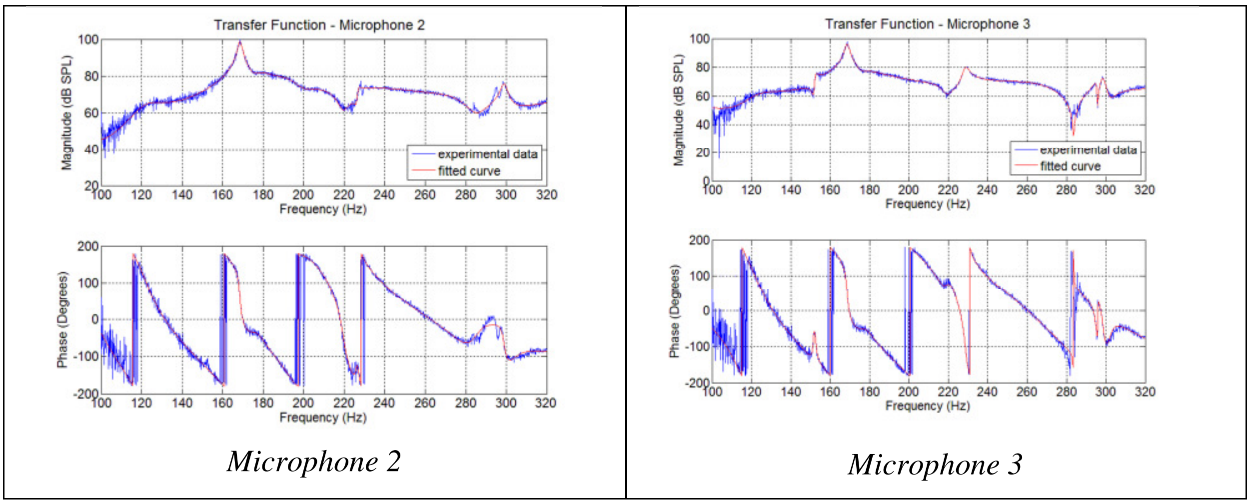

Fig. 5 Experimental and fitted transfer functions of the primary sound source

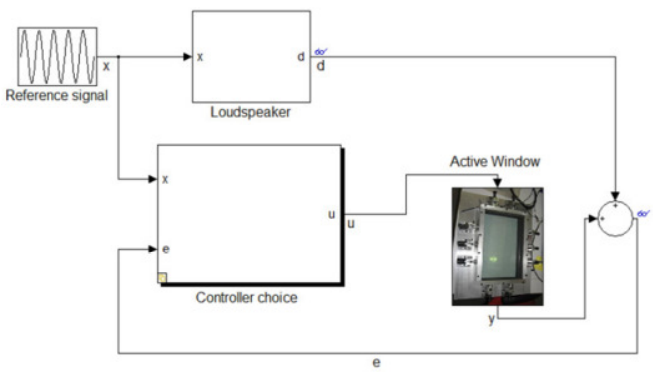

Fig. 6 Block diagram of the multi-channel control algorithms.

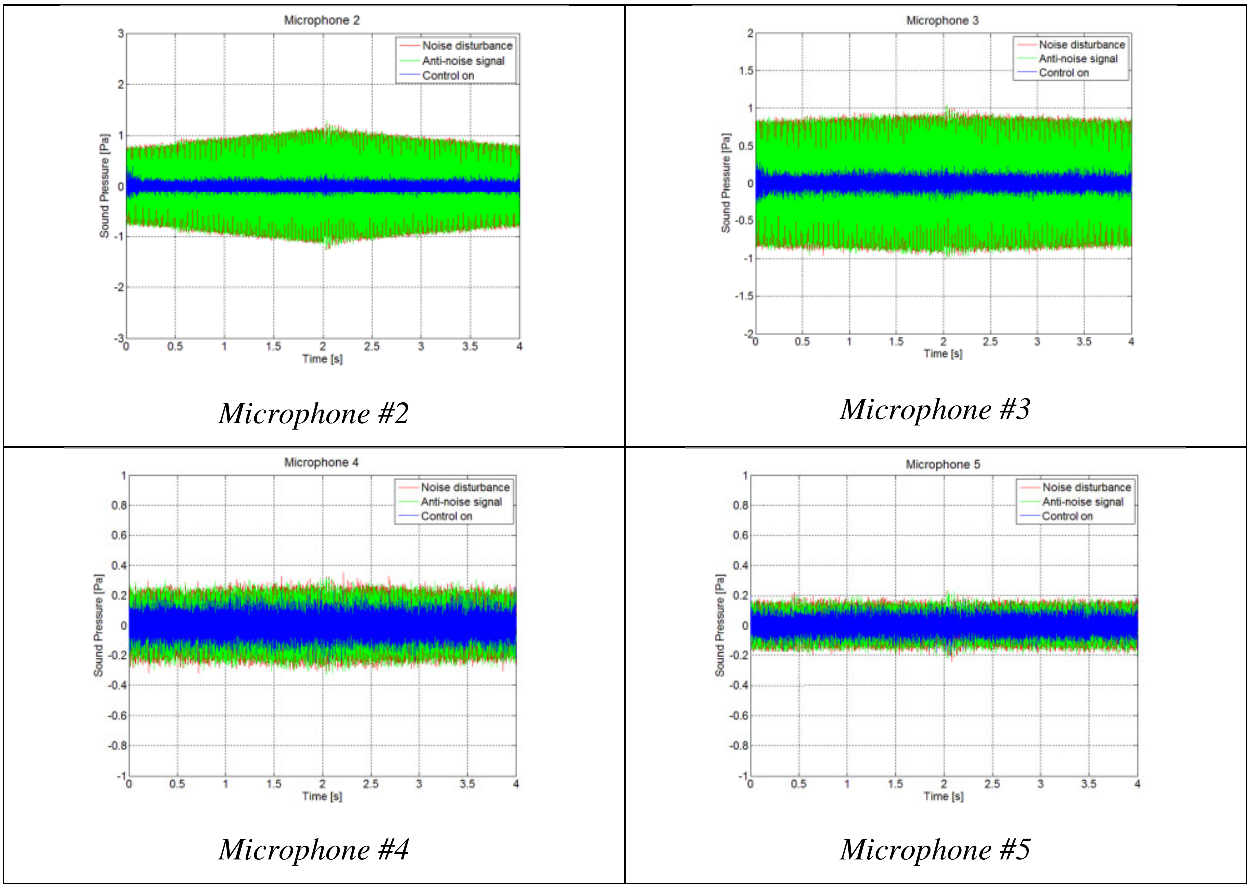

Fig. 7 Numerical predictions of noise attenuation for narrow-band disturbance in the range 80-140 Hz

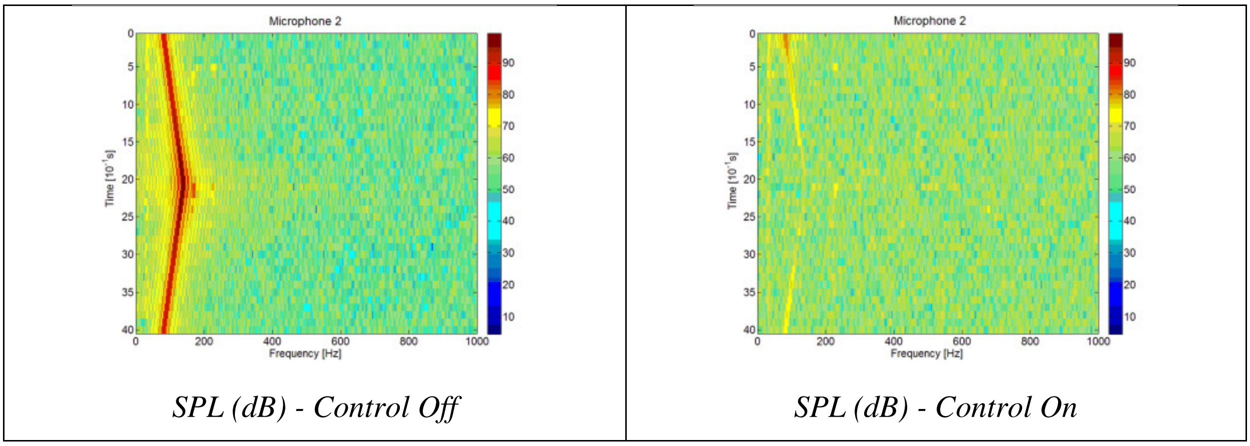

Fig. 8 Performance of the MELMS active control algorithm on a narrow-band excitation: (a) spectogram without control, (b) spectogram with control

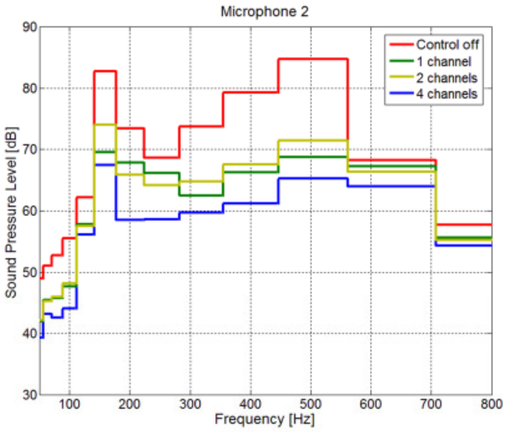

Fig. 9 Sound radiation with and without the active control engaged when the field pressure is minimised at four error sensors with an increasing number of control actuators

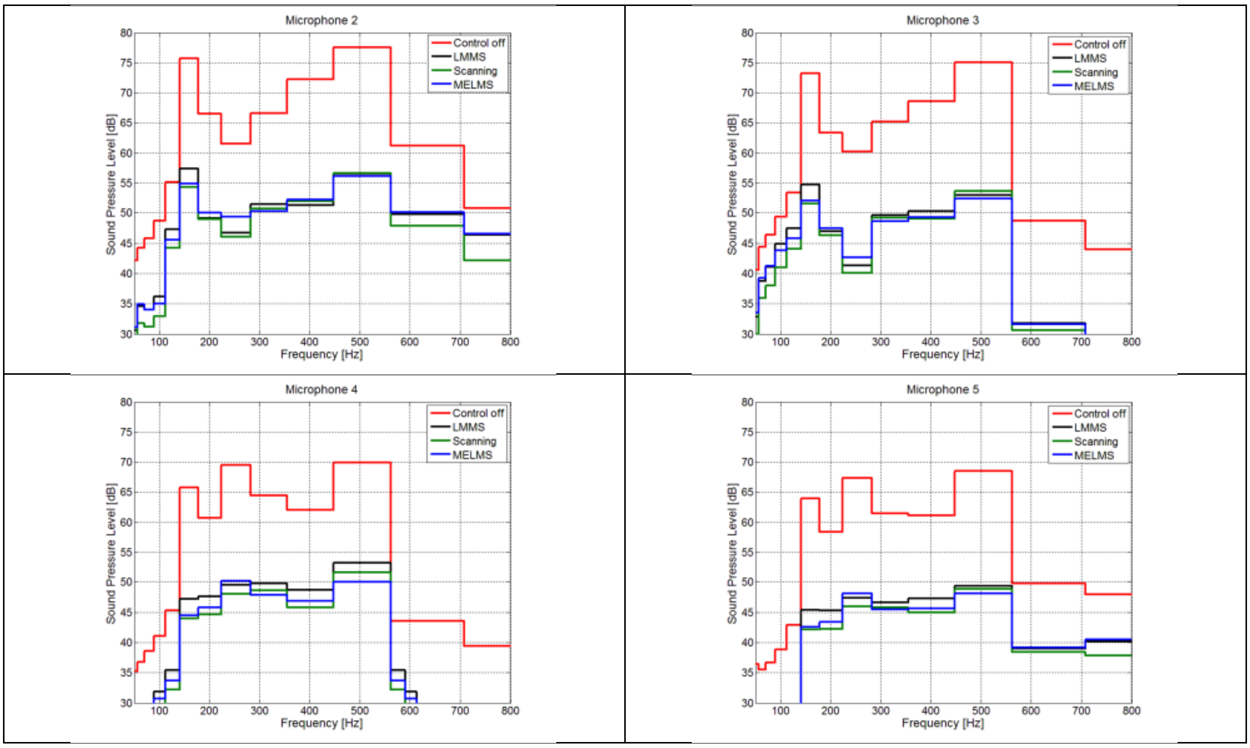

Fig. 10 Third-Octave Sound level attenuation achieved in MIMO systems after the ANC system operation in order to cancel random noise in the range 112-562 Hz. MELMS, LMMS and Scanning error algorithms